

1.2W laser amplification at 1427nm on the 4F3/2 to 4I13/2 spectral line in an Nd3+ doped fused silica optical fiber

J. W. Dawson, P. H. Pax, G. S. Allen, D. R. Drachenberg, V. V. Khitrov, N. Schenkel, M. J. Messerly

August 31, 2016

Optics Express

Disclaimer

This document was prepared as an account of work sponsored by an agency of the United States government. Neither the United States government nor Lawrence Livermore National Security, LLC, nor any of their employees makes any warranty, expressed or implied, or assumes any legal liability or responsibility for the accuracy, completeness, or usefulness of any information, apparatus, product, or process disclosed, or represents that its use would not infringe privately owned rights. Reference herein to any specific commercial product, process, or service by trade name, trademark, manufacturer, or otherwise does not necessarily constitute or imply its endorsement, recommendation, or favoring by the United States government or Lawrence Livermore National Security, LLC. The views and opinions of authors expressed herein do not necessarily state or reflect those of the United States government or Lawrence Livermore National Security, LLC, and shall not be used for advertising or product endorsement purposes.

1.2W laser amplification at 1427nm on the $^4F_{3/2}$ to $^4I_{13/2}$ spectral line in an Nd $^{3+}$ doped fused silica optical fiber

JAY W. DAWSON,^{1,*} PAUL H. PAX,¹ GRAHAM S. ALLEN,¹ DERREK R. DRACHENBERG,¹ VICTOR V. KHITROV,¹ NICK SCHENKEL,¹ AND MICHAEL J. MESSERLY¹

Abstract: A 9.3dB improvement in optical gain and a 100x improvement in total optical power over prior published experimental results from the ${}^4F_{3/2}$ to ${}^4I_{13/2}$ transition in an Nd³⁺ doped fused silica optical fiber is demonstrated. This is enabled via an optical fiber waveguide design that creates high spectral attenuation in the 1050-1120nm-wavelength range, a continuous spectral filter for the primary ${}^4F_{3/2}$ to ${}^4I_{11/2}$ optical transition. A maximum output power at 1427nm of 1.2W was attained for 43mW coupled seed laser power and 22.2W of coupled pump diode laser power at 880nm a net optical gain of 14.5dB. Reducing the coupled seed laser power to 2.5mW enabled the system to attain 19.3dB of gain for 16.5W of coupled pump power. Four issues limited results; non-optimal seed laser wavelength, amplified spontaneous emission on the ${}^4F_{3/2}$ to ${}^4I_{9/2}$ optical transition, low absorption of pump light from the cladding and high spectral attenuation in the 1350-1450nm range. Future fibers that mitigate these issues should lead to significant improvements in the efficiency of the laser amplifier, though the shorter wavelength region of the transition from 1310nm to >1350nm is still expected to be limited by excited state absorption.

OCIS codes: (140.3510) Lasers, fiber; (140.3530) Lasers, neodymium; (140.3280) Laser amplifiers; (060.2320) Fiber optics amplifiers and oscillators.

References and links

- S.B. Poole, D.N. Payne and M.E. Fermann, "Fabrication of low-loss optical fibres containing rare-earth ions," Electr. Lett., 21(17), 737-738 (1985)
- R.J. Mears, L. Reekie, S.B. Poole and D.N. Payne, "Neodymium-doped silica single-mode fiber lasers," Electr. Lett. 21(17), 738-739 (1985)
- L. Reekie, R.J. Mears, S.B. Poole and D.N. Payne, "Tunable single-mode fiber lasers," J. of Light. Tech., LT-4(7), 956-960 (1986)
- 4. E. Desurvire, D. Bayart, B. Desthueux and S. Bigo, *Erbium-doped fiber amplifiers, device and system developments* (Wiley-Interscience, 2002)
- P.C. Becker, N.A. Olsson and J.R. Simpson, Erbium-doped fiber amplifiers: fundamentals and technology (Optics and Photonics), 1st Edition (Academic Press, 1999)
- M.J.F. Digonnet, Rare-earth-doped fiber lasers and amplifiers, Second Edition, Revised and Expanded (Marcel Dekker, Inc., 2001)
- 7. B. Clesca, H. Fevier and W. Pelouch, "Raman Amplification," Opt. and Phot. News, **26**(9), 32-39 (2015)
- 8. S.W. Harun, J. Dimyati, K.K. Jayapalan and H. Ahmad, "An overview on S-band erbium-doped fiber amplifiers," Laser Phys. Lett., 4(1), 10-15 (2007)
- S. Aozasa, H. Masuda, H. Ono, T. Sakamoto, T. Kanamori, Y. Ohishi and M. Shimizu, "1480-1510 nm-band Tm doped fiber amplifier (TDFA) with a high power conversion efficiency of 42%," in *Optical Fiber Communication Conference and International Conference on Quantum Information*, 2001 OSA Technical Digest Series (Optical Society of America, 2001) paper PD1.
- V. V. Dvoyrin, V. M. Mashinsky, L. I. Bulatov, I. A. Bufetov, A. V. Shubin, M. A. Melkumov, E. F. Kustov, E. M. Dianov, A. A. Umnikov, V. F. Khopin, M. V. Yashkov, and A. N. Guryanov, "Bismuth-doped-glass optical fibers—a new active medium for lasers and amplifiers," Opt. Lett. 31, 2966-2968 (2006)
- N. K. Thipparapu, A. A. Umnikov, P. Barua, and J. K. Sahu, "Bi-doped fiber amplifier with a flat gain of 25 dB operating in the wavelength band 1320–1360 nm," Opt. Lett. 41, 1518-1521 (2016)
- D.N. Payne, D. Hewak and E. Taylor, "Progress in the development of efficient 1.3μm fibre amplifiers," in 24th European Conference on Optical Communication, 1998 (Volume: 3), (IEEE, 1998) pp. 9-13

¹ Lawrence Livermore National Laboratory, L-479, P.O. Box 808, Livermore, CA 94550 * dawson17@llnl.gov

- 13. F. Hakimi, H. Po, R. Tumminelli, B.C. McCollum, L. Zenteno, N.M. Cho and E. Snitzer, "Glass fiber laser at 1.36 μm from SiO₂:Nd," Opt. Lett. **14**(19), 1060-1061 (1989)
- I.P. Alcock, A.I. Ferguson, D.C. Hanna and A.C. Tropper, "Tunable, continuous-wave neodymium-doped monomode-fiber laser operating at 0.900-0.945 and 1.070-1.135 μm," Opt. Lett. 11(11), 709-711 (1986)
- P.R. Morkel, M.C. Farries and S.B. Poole, "Spectral variation of excited state absorption in neodymium doped fibre lasers," Opt. Comm. 67(3), 349-352 (1988)
- S. Zemon, B. Pedersen, G. Lambert, W.J. Miniscalco, B.T. Hall, R.C. Folweiler, B.A. Thompson and L.J. Andres, "Excited-state-absorption cross sections and amplifier modeling in the 1300-nm region for Nd-doped glasses," IEEE Phot. Tech. Lett. 4(3), 244-247 (1992)
- W.J. Miniscalco, L.J. Andrews, B.A. Thompson, R.S. Quimby, L.J.B. Vacha and M.G. Drexhage, "1.3μm fluoride fibre laser," Elec. Lett. 24(1), 28-29 (1988)
- Y. Miyajima , T. Komukai and T. Sugawa, "1.31-1.36μm optical amplification in Nd³⁺-doped fluorozirconate fibre," Elec. Lett. 26(3), 194-195 (1990)
- E. Ishikawa, H. Aoki, T. Yamashita and Y. Asahara, "Laser emission and amplification at 1.3μm in neodymium-doped fluorophosphates fibres," Elec. Lett. 28(16), 1497-1499 (1992)
- T. Komukai, Y. Fukasaku, T. Sugawa and Y. Miyajima, "Highly efficient and tunable Nd³⁺ doped fluoride fiber laser operating in 1.3μm band," Elec. Lett. 29(9), 755-757 (1993)
- L. Htein, W. Fan, P.R. Watekar and W.T. Han, "Amplification at 1400-1450 nm of the large-core Nd-doped fiber by white LED pumping," IEEE Phot. Tech. Lett. 25(11), 1081-1083 (2013)
- O. Lumbolt, M. Obro, A. Bjarklev, T. Rasmussen, B. Pedersen, J.E. Pedersen, J. Polvlsen and K. Rottwitt, "Optimum placement of filters in 1300 nm Nd-fibre amplifiers," Opt. Comm. 89, 30-32 (1992)
- M. Naftaly and A. Jha, "Nd³⁺-doped fluoroaluminate glasses for a 1.3μm amplifier," J. App. Phys. 87(5), 2098-2104 (2000)
- D.J. DiGiovanni and K. Rottwitt, "Optical fiber communication system employing Nd doped fiber amplifier for the 1400 nm window," U.S. Patent 6,393,194, Mar 26, 2002
- P.H. Pax, G.S. Allen, D.R. Drachenber, V.V. Khitrov, N. Schenkel, M.J. Messerly, J.W. Dawson, M. Dubinskii, B. Ward, "Scalable waveguide design for three-level operation in Neodymium doped fiber laser," Submitted for publication to Optics Express
- J.W. Dawson, R. Beach, A. Drobshoff, Z. Liao, D.M. Pennington, S.A. Payne, L. Taylor, W. Hackenberg and D. Bonaccini, "Scalable 11W 938nm Nd³⁺ doped fiber laser," in *Advanced Solid-State Photonics, OSA Technical Digest* (Optical Society of America, 2004), paper MD8.
- M. Laroche, B. Cadier, H. Gilles, S. Girard, L. Lablonde and T. Robin, "20W continuous-wave cladding-pumped Nd-doped fiber laser at 910nm," Opt. Lett. 38(16), 3065-3067 (2013)
- 28. T. J. Kane, G. Keaton, M. A. Arbore, D. R. Balsley, J. F. Black, J. L. Brooks, M. Byer, L. A. Eyres, M. Leonardo, J. J. Morehead, C. Rich, D. J. Richard, L. A. Smoliar, and Y. Zhou, "3-Watt blue source based on 914-nm Nd:YVO₄ passively-Q-switched laser amplified in cladding-pumped Nd:fiber," in *Advanced Solid-State Photonics (TOPS)*, G. Quarles, ed., Vol. 94 of OSA Trends in Optics and Photonics (Optical Society of America, 2004), paper 160.
- D.B.S. Soh, S.Yoo, J. Nilsson, J.K. Sahu, K. Oh, S. Baek, Y. Jeong, C. Codemard, P. Dupriez, J. Kim and V. Philippov, "Neodymium-doped cladding pumped aluminosilicate fiber laser tunable in the 0.9-μm wavelength range," IEEE J. of Quant. Elec. 40(9), 1275-1282 (2004)
- C. Bartolacci, M. Laroche, T. Robin, B. Cadier, S. Girard and H. Gilles, "Effects of ions clustering in Nd³⁺/Al³⁺-codoped double-clad fiber laser operating near 930nm," Appl. Phys. B, 98, 317-322 (2010).
- 31. F. Luan, A.K. George, T.D. Hedley, G.J. Pearce, D.M. Bird, J.C. Knight and P.St.J. Russell, "All-solid photonic bandgap fiber," Opt. Lett. 29(20), 2369-2371 (2004).
- A. Cerqueira S. Jr., F. Luan, C.M.B. Cordeiro, A.K. George and J.C. Knight, "Hybrid photonic crystal fiber," Opt. Express 14, 926-931 (2006).

1. Introduction

Fiber lasers and amplifiers are the subject of significant research and have been since University of Southampton demonstrated the potential for low loss rare earth doped optical fibers in 1985 [1] and subsequently gain and lasing in both Neodymium and Erbium doped silica optical fibers [2, 3]. The primary driver of research efforts in optical fiber amplifiers in the late 1980s and early 1990s was the major impact on bandwidth of fiber optic communication systems enabled by wavelength division multiplexing and erbium fiber amplifiers. Optical fiber amplifiers enable long haul transmission of many optical channels without the high cost of detecting each individual channel, electronically amplifying and then modulating a laser and recombining the channels every 15-20km. Instead, a single erbium fiber amplifier restores the optical signal power across all transmission channels in a single compact, efficient and low cost device. C and L band erbium fiber amplifiers provide amplification across 1525 nm to 1620 nm. WDM channel spacing as small as 50 GHz enables a single optical fiber to achieve an information carrying capacity on the order of Tb/s. Early

research in erbium fiber amplifiers is well summarized in a number of books specifically on this topic [4-6] and these amplifiers are now technologically mature.

During the same time period when erbium fiber amplifiers were being developed significant R&D was also put into developing a rare earth doped fiber amplifier in the 1300-1500nm-telecom window referred to as the O, E and S-bands. However, amplifiers in this wavelength range have not had the same commercial impact due to efficiency concerns or because they are based upon non-fused silica glasses, which are generally perceived to be more difficult to integrate into the fiber optic network due to differences in the material properties between them and the fused silica material of the rest of the network.

Fiber amplifiers at wavelengths from 1300 nm to 1530 nm fall into several categories. Raman amplifiers [7] are the top contenders and can attain a wide array of wavelengths as amplification occurs 13.2 THz from the pump wavelength, which can be picked arbitrarily. However, Raman amplifiers require long fiber lengths and high power pump lasers. S-band fiber amplifiers based upon erbium and thulium have been studied extensively [8, 9]. In the erbium case, depressed well fiber geometries are employed to suppress the much higher gain at >1530 nm, but require operating at very high inversions as the emission cross section is significantly less than the absorption cross section at these wavelengths in addition to added losses and fabrication challenges imposed by the depressed well waveguide design. In the thulium case R&D has focused on non-fused-silica fibers as the decay from the upper level laser state is faster than the decay from the lower state making this laser transition self terminating in fused silica. Recently, bismuth doped fiber amplifiers have emerged as a possible fiber amplifier in the 1320-1360nm region [10, 11]. However, these amplifiers remain relatively low in optical efficiency and require long fiber lengths. Praseodymium and neodymium were extensively researched [12] for amplification in the E and O band (1300-1450nm). Praseodymium worked well only in fluoride based fibers.

Neodymium doped fiber lasers and amplifiers in the 1320-1450nm-wavelength range [13] would appear to have some significant attractions as this transition line ${}^4F_{3/2}$ to ${}^4I_{13/2}$ is a 4-level laser line and thus has no ground state absorption issues. Figure 1 below, a simplified energy level diagram of the relevant Nd³⁺ transitions, is included for easy reference. However, this transition also has significant drawbacks that have limited its utility. First in fused silica as well as other materials there is a well-known excited state absorption (ESA) from the ⁴F_{3/2} state [14-16] that creates a net optical loss when the laser amplifier is pumped, especially in the region from 1300-1350nm. The status of the 1350-1390nm region is less clear as it appears to be convolved with the 1380nm spectral absorption due to OH in many reports. Even with these limitations, net gain (10 dB) and lasing (~10mW) has been demonstrated [13, 17-21] though positive gain occurs well beyond the fluorescence peak where the emission cross section is highest. The lower cross sections complicate the other key challenge of operation on the ${}^4F_{3/2}$ to ${}^4I_{13/2}$ transition, which is competition from the preferred transitions ${}^4F_{3/2}$ to ${}^4I_{9/2}$ and ${}^4F_{3/2}$ to ${}^4I_{11/2}$. It has been proposed [22-24] that spectral filtering of the ⁴F_{3/2} to ⁴I_{11/2} transition would improve performance of a neodymium-doped fiber on ⁴F_{3/2} to ⁴I_{13/2} transition, but to our knowledge spectral filtering has never before been demonstrated experimentally for this transition.

In this paper we report the first experimental demonstration of a neodymium doped fused silica optical fiber amplifier operating on the ${}^4F_{3/2}$ to ${}^4I_{13/2}$ transition employing a continuous spectral filter of the ${}^4F_{3/2}$ to ${}^4I_{11/2}$ transition while still guiding light in the wavelength range from 1300-1500nm. To the best of our knowledge, the 1.2W amplified power at 1427nm reported here is two orders of magnitude greater than prior published fiber lasers operating on this transition [17, 20]. Further, the 19.3 dB small signal gain reported here is 9.3dB higher than the best previous neodymium fiber amplifier result [18] on this transition.

The above review of the literature has predominantly discussed telecom applications. The fiber amplifier reported in this work is a double clad Nd^{3+} optical fiber with a $20\mu m$ core. This design is not consistent with a telecom type amplifier that would optimally have a smaller

core diameter and operate at lower power levels and shorter amplifier lengths. The fiber reported upon in this work was originally intended for generation of high power light in the wavelength range from 900 nm to 940 nm and its operation in this wavelength range is reported in detail elsewhere [25]. During the course of testing this fiber for its originally intended purpose, significant amplified spontaneous emission was observed in the 1400 nm wavelength region. Based upon the prior reports [13-21], it was recognized that this behavior was not expected. To that end, a set of experiments to investigate the potential for gain in this region was designed, executed and are reported on here. We recognize that this fiber is not suitable for use as a telecom amplifier as built. In particular, the overall efficiency of the fiber is too low for this purpose. However, the results reported here suggest that an optimized fiber with significantly lower background loss, a 2-4x smaller core diameter and additional waveguide features to eliminate amplified spontaneous emission from 850 nm to 1150 nm may perform significantly better from the standpoint of efficiency. Such a fiber might be directly core pumped and attain significant gain over a much shorter length. Note these potential benefits are speculative at this point in time. The remainder of this paper reviews our fiber design and current limitations and the experimental set-up employed to demonstrate gain and amplification at 1427 nm.

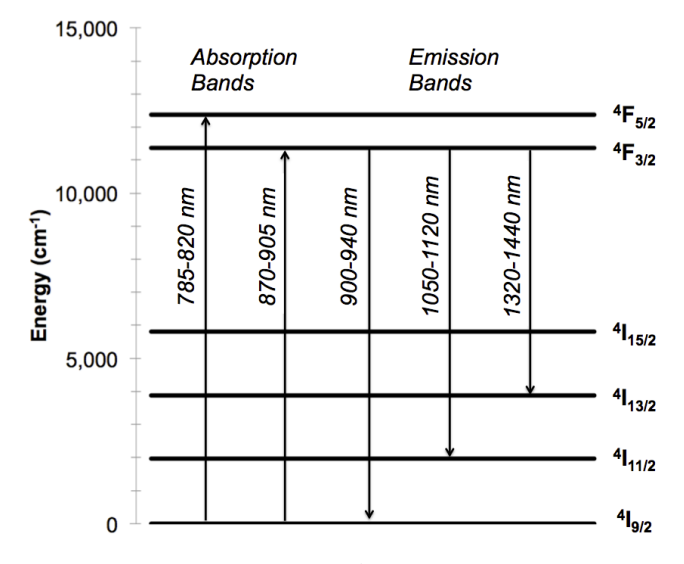


Fig. 1: Simplified energy level diagram for Nd³⁺ in fused silica. Each energy level is a homogeneously broadened multiplet of states. The absorption and emission wavelengths are denoted as a band rather than only noting the peak in order to reflect the wide wavelength range of emissions represented by each pair of energy levels.

2. Nd³⁺ optical fiber with continuous spectral filtering

The results presented here employ a Nd^{3+} doped optical fiber developed for amplifiers and lasers in the 900-930nm wavelength range [25]. We have been seeking to improve over prior designs that rely either upon large core to clad ratio [26, 27] or a depressed well geometry [28, 29]. The large core to clad ratio scheme is limited in overall pump cladding size by the requirement the pump cladding diameter not be much bigger than 4x the core diameter. The depressed well scheme is limited to <10 μ m in core diameter by the requirement the 1 μ m light be able to tunnel through the depressed well into the cladding. Thus as the pump cladding is progressively increased the fiber becomes progressively longer in order to be efficient. Our design uses recent advances in micro-structured optical fibers to overcome these limitations.

A picture of the end face of our fiber is shown in fig. 2 below. The overall fiber is round and the outer glass diameter is 240µm, the inner pump cladding is hexagonal with a face-to-

face dimension of $118\mu m$ and a corner-to-corner dimension of $136\mu m$. The core is also hexagonal with a face-to-face dimension of $21\mu m$ and a corner-to-corner dimension of $24\mu m$. The micro-structure comprising the core and pump cladding was fabricated from a stack of 217 canes, 17 canes corner to corner that are surrounded by tubes that are pressurized with air during the draw process to form a pump cladding with an NA of 0.4 at 880nm. As fabricated the pitch of the micro-structured elements is $8\mu m$.

The inner rod and 1st inner ring (7 elements) is Nd³⁺ doped glass matched in refractive index to fused silica. This was achieved by procuring a Nd³⁺ doped preform with large core to clad ratio from Optacore SA that had an initial doping level corresponding to 200dB/m of absorption at 808nm and likely in the realm where there is significant concentration clustering of the Nd³⁺ ions [30]. Canes drawn from this preform were incorporated into a stack and draw preform that contained additional silica and fluorinated rods drawn from other preforms. This assembly was designed such that the area weighted refractive index of all components was matched to that of the refractive index of fused silica to <10⁻⁴, though we lack the ability to verify the end product via measurement and rely solely upon the design to estimate the index. The assembly was then drawn into rods, restacked and drawn again to further reduce the feature size. The final rods were incorporated into the preform that produced the fiber in fig. 2 and we estimate that the feature sizes of the final rods are on the order of 125nm. We estimate the effective concentration of Nd³⁺ ions was reduced by 5x due to this process i.e. 40dB/m at 808nm. It is not known whether the process had any impact on the probable clustering we suspect existed in the original preform.

The next four rings of the microstructure are a combination of fluorinated depressions and GRIN inclusions. The fluorinated depressions are 0.533 center to outside ratio with an index depression of -0.0068 relative to fused silica and are incorporated in lieu of air holes making the structure easier to fabricate and easier to handle as the final structure has the potential to be all-solid. The fluorinated depressions define the waveguide and are seen in fig. 2 as darkened spots. The 18 bright spots radiating from the corners of the core are GRIN inclusions fabricated from a commercial GRIN preform suitable for fabricating 62.5/125µm standard multimode GRIN fiber. These inclusions are resonant with the core in the 1020-1130nm wavelength range and draw light at these wavelengths out of the core and leak it into what is effectively a reservoir of a large number of modes formed by the outer three rings of the pump cladding. The rods that form the fluorinated depressions and the GRIN inclusions were obtained as bulk preforms fabricated via plasma chemical vapor deposition (PCVD) from Prysmian and drawn into canes for incorporation into the final preform. The outer region is formed from Hereaus F300 fused silica rods.

The filtering effect of the GRIN inclusions is subtly different from traditional all-solid photonic band gap structures [31]. We note the design is similar in structure to hybrid photonic crystal fibers [32] suggests the GRIN inclusions act as an Anti-Resonant Reflecting Optical Waveguide (ARROW), where light in resonance is coupled out of the core and is reflected back into the core if it is anti-resonant. The design here is subtly different than the hybrid photonic crystal fiber in that a fluorinated barrier is included between the core and the first GRIN inclusion. Our view [25] is that the mode is stably guided by these fluorinated depressions, except at certain wavelengths where a resonant bridge is formed by the GRINs between the core and the reservoir formed by the pure silica region between the waveguide structure and the pump cladding. Scattering of the light in this reservoir mixes it into many modes reducing back-coupling into the core via the same route. The mechanism of resonant coupling of certain wavelengths in the core to the outer reservoir creates high loss in the range from 1050 nm to 1120 nm, reducing the build-up of amplified spontaneous emission on the 1064 nm line.

The microstructure is surrounded by a final ring of capillary holes that can be pressurized during the draw process to enable the formation of a pump cladding with a numerical aperture of ~0.4 at 880nm. Fiber samples with and without capillary holes were drawn. The samples

without capillary holes were useful for assessing core spectral attenuation. The samples with capillary holes were used in the laser and amplifier experiments described below. As the filtering aspect of the waveguide does not rely upon air-holes, replacement of the air-holes for the pump cladding with a standard low-index polymer coating would enable this design to be all-solid, which would have significant handling advantages.

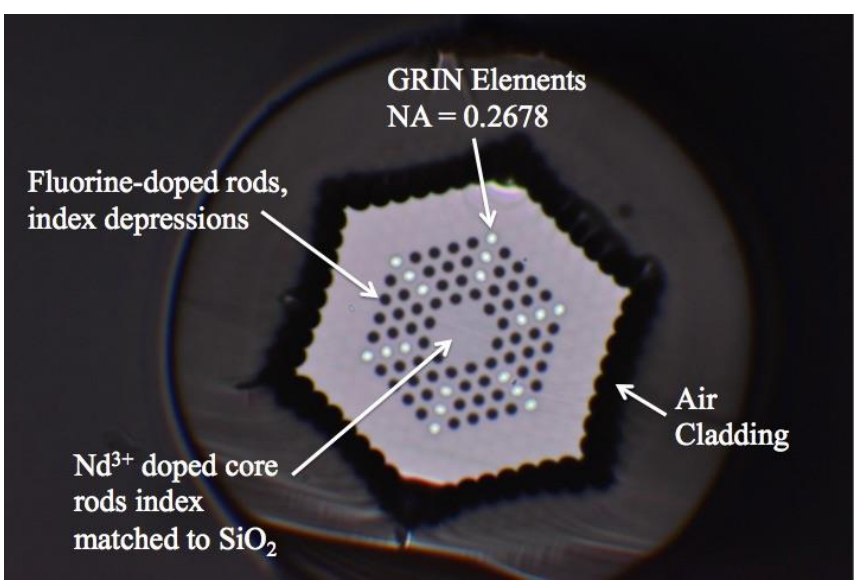


Fig 2. End-face of Nd³⁺ doped fused silica fiber employed in this work

Figure 3 shows the measured spectral attenuation of the single clad version of the fiber shown in fig. 2 above. The attenuation below 950nm was too high to measure due to the Nd³⁺ ground state absorptions. The spectral attenuation was measured using a super-continuum white light source, a monochrometer, a lock-in amplifier and photo-detectors via the standard cut-back technique with the exception that the end face was imaged onto an iris preceding the photo-detector that blocked light guided by the GRIN inclusions. Two measurements were made; the red line in fig. 3 was derived from a cutback on a short piece of fiber that permitted assessment of the high (~10dB/m) attenuation region between 1020nm and 1130nm. A cutback on a longer piece permitted assessment of the losses outside this region, blue dotted line. For reference the black solid line with greater dynamic range is the theoretical estimate of the anticipated attenuation of the waveguide in the 1020-1130nm wavelength region.

In addition to the desired high spectral attenuation in the 1020-1130nm-wavelength range, the fiber exhibits an abnormally high 1380nm OH peak of 1dB/m or 1000dB/km. The original Optacore Nd³+ doped glass did not contain an OH peak of this magnitude. We estimate the OH peak of the starting glass to be much smaller (<50dB/km). We believe the core glass was contaminated with OH during the extensive processing to match its index to fused silica. We do not believe this contamination is intrinsic to the process and are examining our procedures to minimize this contamination in future fibers. We strongly believe the high OH peak is preventable and is limiting the results reported below. The spectral attenuation measurement suggests a core loss of 0.27dB/m at 1427nm (the wavelength at which our amplifier experiments below are performed). However, a direct cutback using the seed laser suggests the actual losses are closer to 0.18dB/m at this wavelength. We believe this discrepancy to be within the error of our loss measurement, which was done on a relatively short length of fiber (~100m). The loss (equivalent to 180dB/km) is still extremely high for an optical fiber and certainly limiting the laser amplifier results in a number of ways.

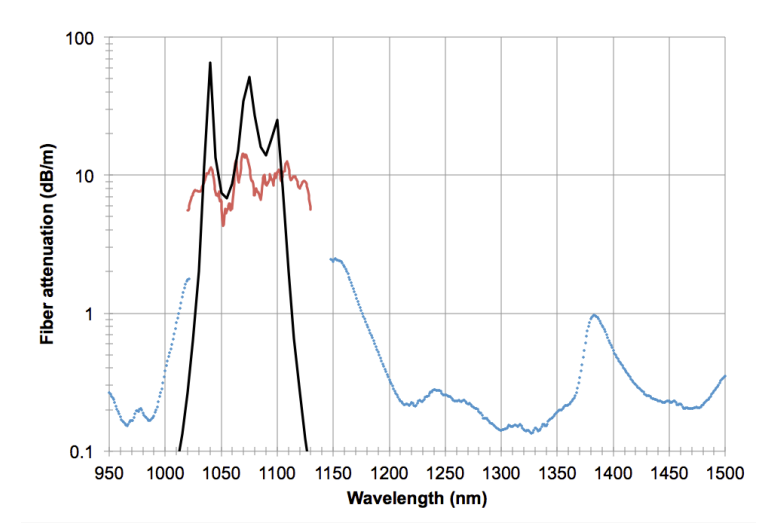


Fig. 3: Spectral attenuation of core of Nd³⁺ doped optical fiber (red line) short cutback 1020-1130nm, (blue dotted line) long cutback, (black solid line) theoretical model.

The pump cladding absorption was measured via the cutback technique on a double clad sample of the fiber and the results are shown in fig. 4 below. The absorption is roughly 1/3rd of what we estimate it should be based upon the expected core absorption and the pump cladding-to-core area ratio of 31. One may be concerned the GRIN inclusions are trapping pump light. However, the GRIN inclusions are only 1% of the total effective area of the pump cladding region. The low pump absorption is suspected to be a result of light being partially trapped in the silica region between the outermost ring of fluorinated depressions and GRIN inclusions and the air cladding. This effect is discussed in greater detail elsewhere [25].

The 808 nm absorption peak, the most common Nd³⁺ pump wavelength, is 0.39 dB/m. A 30m length of fiber will absorb roughly 11.7dB of 808nm pump light. The 880nm absorption peak which absorbs light directly into the ⁴F_{3/2} upper level laser state is only 0.2dB/m absorption meaning a 60m piece of fiber is required to attain the same small signal pump absorption. It will be shown in the next section that despite the longer length, the 880nm pump absorption peak is preferred in this fiber for lasing on the ${}^{4}F_{3/2}$ to ${}^{4}I_{13/2}$ transition because it reduces the average inversion of the fiber, which minimizes amplified spontaneous emission on the ${}^{4}F_{3/2}$ to ${}^{4}I_{9/2}$ transition at 900-940nm, which is a limit on our current results. Once this transition is also suppressed, in the next fiber iteration, the 808nm pump line may be preferred as fibers ½ the length can be employed to attain the same pump absorption. Also called out in fig. 4 is the pump absorption at 913nm. We attempted core pumping of the fiber with 2W of pump at both 910nm and 923nm using a separate piece of this fiber lasing at these wavelengths. However, we saw no signs of gain on the ${}^4F_{3/2}$ to ${}^4I_{13/2}$ transition when the fiber was pumped at these wavelengths. We tentatively conclude that the attainable inversions at these wavelengths are insufficient to provide enough gain to overcome the 0.17dB/m core loss in this fiber sample. To this end, we considered, but did not attempt cladding pumping of the fiber at 915nm.

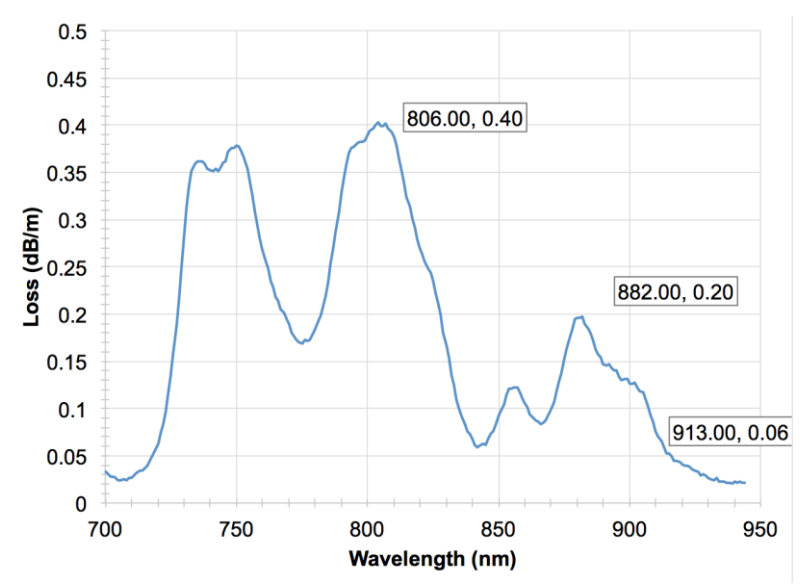


Fig. 4: Measured absorption of the pump cladding.

3. Amplified spontaneous emission vs. pump power

Figure 5 illustrates the baseline experimental set-up for testing the fiber. We performed two sets of tests. Reported in this section are measurements of the fluorescence spectrum from the core of the fiber as a function of coupled pump power. Reported in the next section (section 4) are gain and power measurements from the seeded fiber amplifier. The fiber was pumped with an 880nm Dilas laser diode coupled to a 200μm/0.22NA multimode optical fiber. A 40mm focal-length plano-convex lens from Thorlabs with a B-type AR coating collimated the output of this diode. The pump light was passed through an iris to limit the numerical aperture of the light coupled to the fiber. The pump light was then reflected off two Semrock long pass filters at 35° angle of incidence in order to separate the output of the fiber from the pump light and minimize transmission of light from the fiber back into the pump laser diode. At 35° angle of incidence, the Semrock filter's 50% reflectivity point is at 900nm. The pump light was then coupled into the neodymium fiber using a 20mm focal length aspheric lens from Thorlabs again with a B-type AR coating that we measured to have transmission of 88% at 1427nm.

We prepared the pump end of the neodymium fiber by collapsing the air holes forming the pump cladding using an optical fiber fusion splicer and then angle cleaving (\sim 10°) the fiber as close as possible to the end of the region with inflated holes. Coupled pump power was determined via direct measurement by cutting the fiber to 2m at the completion of testing. Due to the method by which the fiber input was prepared, the output from the fiber core was not well collimated by the input lens when the pump coupling was optimized. To compensate for this, an additional 500mm focal length C-coated biconvex lens from Thorlabs was positioned approximately 355mm from the 20mm input lens. This re-imaged the fiber end onto the first iris at approximately 520mm from the 500mm lens. This iris was employed to screen out fluorescence guided by the pump cladding. A second iris 250mm further down the beam path was employed to block non-core light making it through the first iris. For the purpose of the experiments reported in this section (section 3), the core light was then coupled into an SMF-28 fiber using an 8mm Thorlabs C-coated asphere and connected to an optical spectrum analyzer for assessment of the fluorescence spectra of the fiber. The output end of the fiber was terminated similar to the input end and a power meter was employed to optimize the pump coupling. The rest of the experimental set-up will be described in the next section. Note that fig. 5 shows the core beam as being coupled to a power meter, however this was done for the power and gain testing, not for the fluorescence measurements.

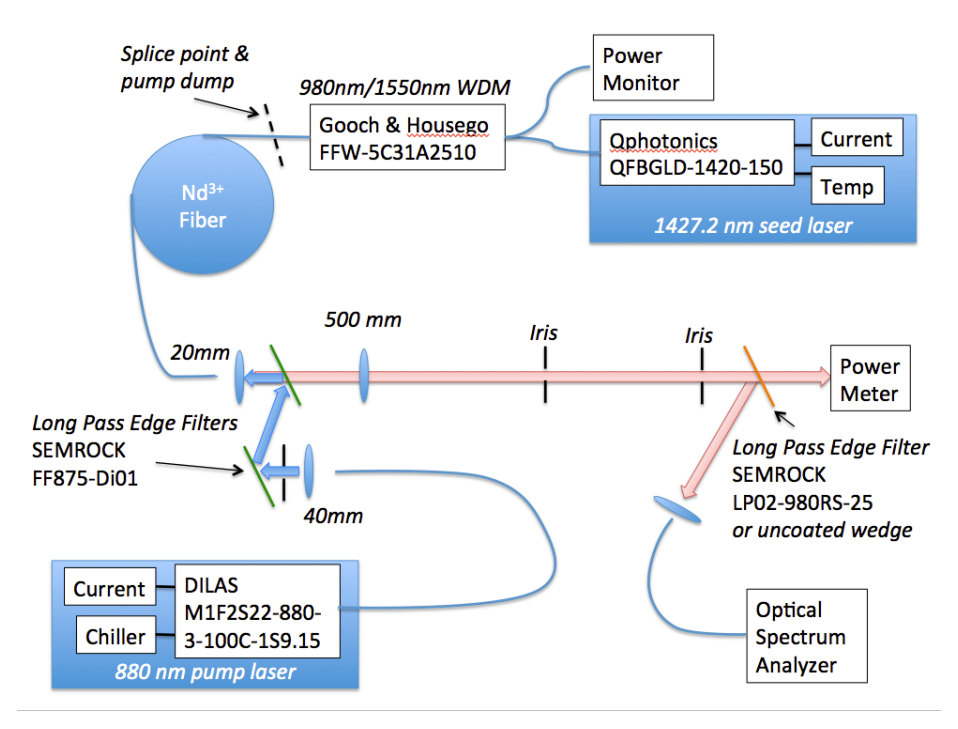


Fig. 5: Block diagram of experimental set-up

Figure 6 plots the fluorescence spectra as function of coupled 880nm pump power from the output of a 60m-neodymium fiber sample. As expected for this fiber, a strong increase in the 930nm fluorescence as a function of pump power is observed. The fluorescence intensity at 930nm for 12.7W pump power is 1860x stronger than the fluorescence intensity at 0.37W pump power. As the pump power has increased by only 34.3x this is a clear sign of amplified spontaneous emission at 930nm. In the 1050-1150nm wavelength range a similar comparison of fluorescence intensity reveals only a 56x increase in fluorescence intensity suggesting little or no net gain in this region. (There was some regrettably unavoidable alignment drift between the neodymium fiber and the single mode fiber coupling light to the core during the measurement due to heating of the fiber mount by uncoupled pump light. The curves were taken starting with the highest power and then successively decreasing the power. Thus alignment was best at the highest power and likely slightly worse at the lowest power. We believe this to be the reason the fluorescence intensity appears to increase slightly faster than the pump power across the spectrum.) This is consistent with our assertion that the waveguide design has spectral attenuation in the 1050-1150nm wavelength range sufficient to fully suppress the expected gain. Similarly the fluorescence peak at 1337nm shows only a 56x increase in total intensity again consistent with no net gain, this is most likely due to excited state absorption [14-16]. However, the wavelength region from 1380-1450nm is evolving very differently from the 1330-1380nm wavelength region. The fluorescence spectra in this region is clearly increasing non-linearly with pump power and at both 1400nm and 1420nm the fluorescence increases by 186x compared to the initial fluorescence power. This is 10x less than the increase at 930nm, but still sufficiently high to conclude there is amplified spontaneous emission (ASE) in this wavelength region.

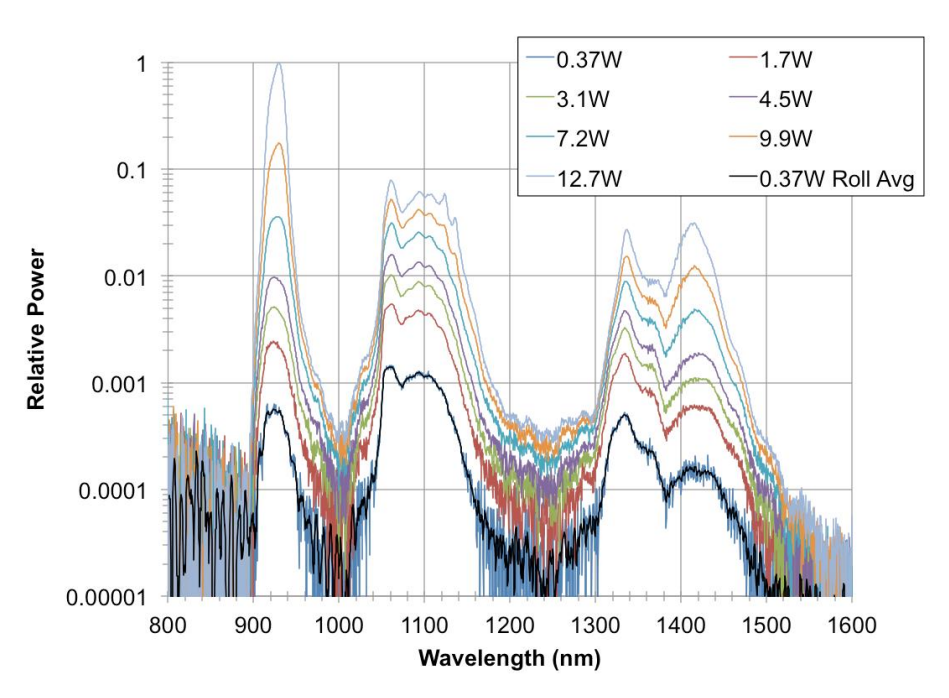


Fig. 6: Core fluorescence as a function of coupled 880nm pump power

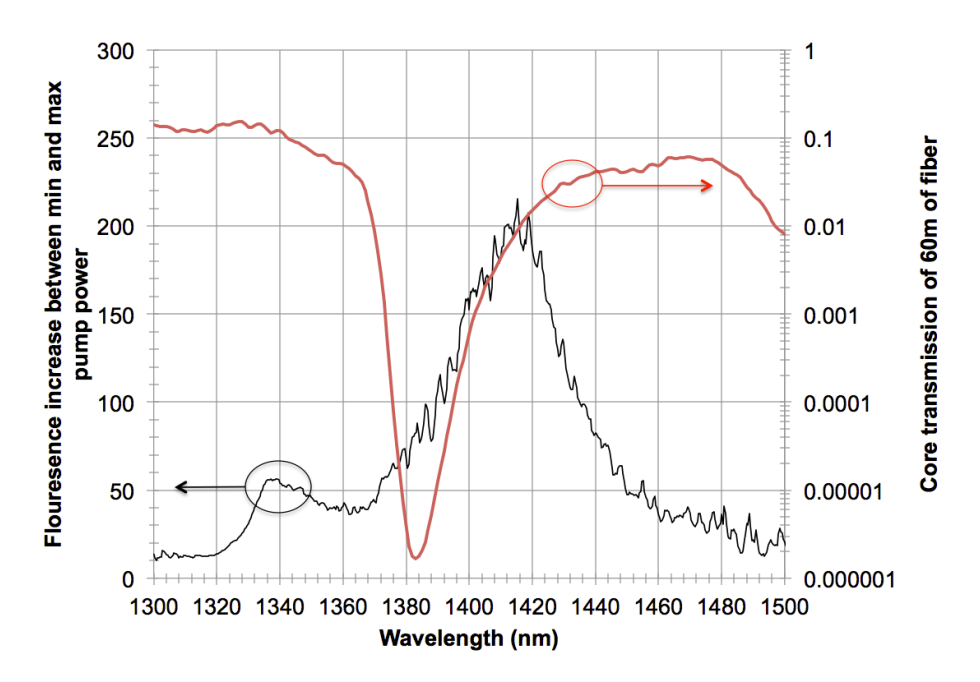


Fig 7: Increase in fluorescence in the 1300-1500nm wavelength region for an increase in pump power of 34.3x (0.37W to 12.7W coupled pump at 880nm into a 60m long fiber), black line. The core transmission of a 60m long fiber (red line) is plotted on the second y-axis to illustrate the rapidly changing fiber loss in this wavelength region. We assert that an increase of >60 in fluorescence in this fig. is convincing evidence of net gain.

Figure 7 plots the ratio of the fluorescence intensity measured at 12.7W coupled pump power to the rolling average of the measured fluorescence intensity at 0.37W of coupled

pump power (black line, left vertical axis, linear range). In order to highlight the effect of the OH induced loss in this particular fiber sample, the spectral attenuation data from fig. 3 was used to calculate the net transmission of a 60m length of this neodymium fiber (red line, right vertical axis, logarithmic range). Based upon our estimates of the increase in the fluorescence in the regions where we do not expect net gain is ~56x, we assert that regions of the plot where the increase in the fluorescence intensity is >60x denotes the region of positive gain. Note there is a strong correlation between the rising gain from 1370nm to 1414nm and the exponentially rising fiber transmission in the same region. This suggests an improved fiber with reduced OH will be capable of significant gain possibly as short at 1360nm. Thus an improved neodymium fiber based upon this design may have an amplification window as large as 80nm.

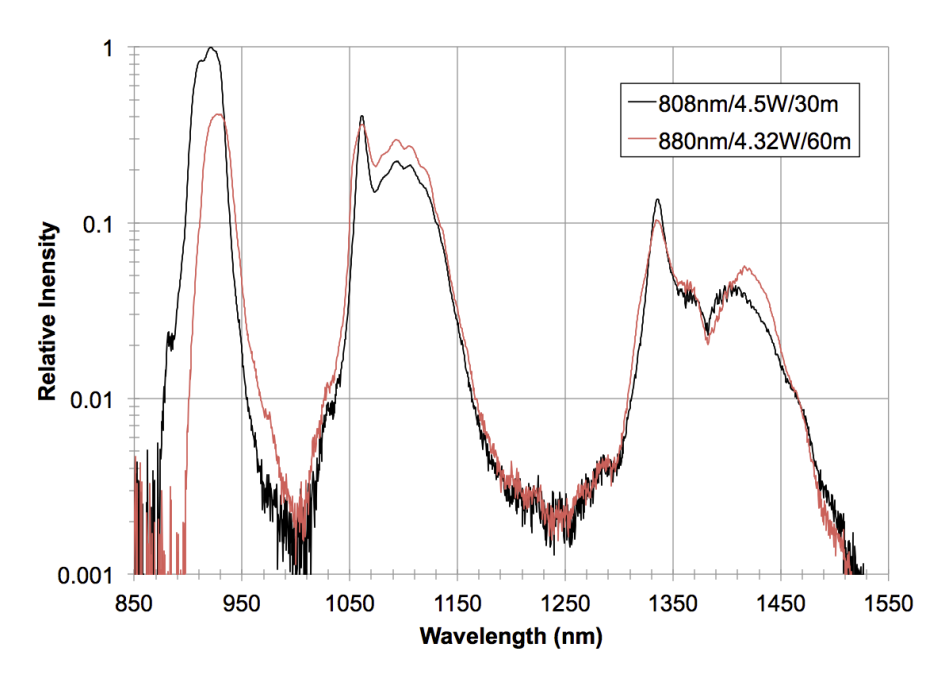


Fig. 8: Comparison of neodymium fiber fluorescence for 808nm and 880nm pumping at same nominal pump power and same nominal small signal absorption from the cladding (~11.7 dB).

We conclude this section with fig. 8, which compares the fluorescence spectrum from the core of this fiber for 4.32W coupled pump power at 880nm into a 60m long fiber (note this curve was taken on a different day than the fig. 7 data) to the fluorescence spectrum from the core of another piece of fiber that is 30m long and pumped with 4.5W of coupled 808nm diode laser light. In this case, the Dilas laser diode in fig. 5 was replaced by a LIMO laser diode (LIMO25-F100-DL808). The LIMO laser diode was coupled to a 100 µm/0.22NA core fiber and the Semrock filters were adjusted to 45° angle of incidence to move the 50% transmission point to 875nm. The different neodymium fiber lengths were chosen in order to equalize the pump absorption in the two cases. As the fluorescence spectra were taken on different days using different experimental arrangements, we normalized both curves to 1 at their fluorescence peaks and then uniformly attenuated the 880nm data in order to align the fluorescence power from the two curves in the region between 975nm and 1300nm. Figure 8 illustrates clearly that the 900-950nm fluorescence peak is much stronger for the 808nm pump than the 880nm as one would expect due to both improved transmission of the dichroic filter and due to the higher average inversion in the fiber. However, the fluorescence spectrum between 1380nm and 1450nm shows superior gain on the ⁴F_{3/2} to ⁴I_{13/2} line for the 880nm pump. We attribute this to lower average inversion and thus less power is lost to the ⁴F_{3/2} to $^4I_{9/2}$ transition improving the gain on the transition we are investigating. We contend an improved fiber with deliberate spectral attenuation from 850-1150nm, when combined with reduced OH as discussed above, will enable significant gain in the 1360-1440nm range.

4. Direct measurement of gain and power at 1427 nm

Referring again to fig. 5, once the fluorescence spectrum measurements shown in fig. 6 were completed, a 1427nm diode laser source was launched into the core of the 60m piece of neodymium fiber counter-propagating to the direction of the pump laser. An optical isolator was not available for this diode laser. In order to protect the laser from significant backward propagating light in the 900-950nm wavelength range the output of the diode laser was fusion spliced to a standard 980/1550nm telecom wavelength division multiplexer (WDM) used for the construction of erbium doped fiber amplifiers. The measured insertion loss of the WDM was 3dB at 1427nm and 1.2dB at 905nm. The 980nm port of the WDM was aligned to an optical power meter to permit a relative assessment of backward propagating light in the 900-950nm region during the tests. The output of the WDM was fusion spliced directly to the neodymium fiber and the splice was potted into a copper V-groove using a high index optical quality polymer. This assembly provided a convenient place to dump excess pump light transmitted through the neodymium fiber. We note that the WDM is made from HI 1060 FLEX fiber which is not well mode-matched to the 20µm, low NA core of this neodymium fiber. Thus we anticipated and measured very high splice loss. The splice loss was calibrated at the end of the measurement campaign by cutting the fiber length back to 2m and measuring the collimated 1427nm signal using the fiber launch, lenses and irises shown in fig. 5.

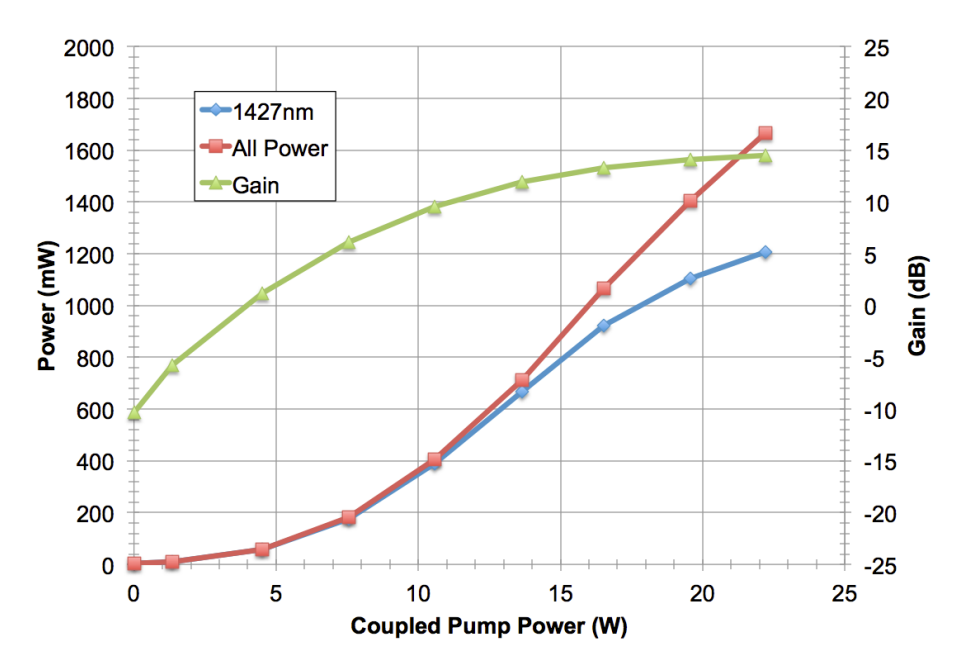


Fig. 9: Power and gain vs. coupled pump power for 43mW of 1427nm launched signal light.

As noted in fig. 5, the light from the output of the neodymium fiber was stripped of stray cladding light using two irises and then measured with an optical power meter. Output power vs. pump power was measured both with and without a Semrock LP02-980RS-25 long pass filter, which has 50% transmission at 980nm for 45° angle of incidence. This filter enabled measurement of only power longer than 980nm eliminating the strong ASE in the 900-950nm

wavelength region observed at high pump power. When the Semrock filter was not in line, an uncoated fused silica wedge was put in its place and the light from the front surface reflection was coupled to an SMF-28 fiber and then to an optical spectrum analyzer.

Figure 9 plots measured power vs. coupled pump power for the case of the LP02-980RS-25 filter in place (blue line, 1427nm power) and the case of the uncoated wedge in the filter's place (red line, All power). The loss of these filters was accounted for in the data analysis. The gain was then computed based upon the launched 1427nm power of 43mW. The maximum output power was limited by the onset of parasitic lasing at 930nm. The 1427nm power effectively clamped at this point and we did not proceed to increase the pump power further due to concerns about damaging the seed laser. Points containing 930nm parasitic lasing are not plotted. The backward propagating 900-950nm light measured out of the 980nm port of the WDM was 45mW at the max output power. This is an uncalibrated value and may contain significant 1120nm power. Figure 10 plots the spectra for selected points shown in fig. 9 as well as the integrated power vs. wavelength for the 1205mW (highest power) data point. We see from fig. 10 that ~20% of the power at the highest measured value was in the 920nm ASE consistent with the ~25% difference between the blue and red curves in fig. 9.

The 1.1µm wavelength band is <1% of the total power and thus even though the 980nm edge filter does not block this light, the contribution of 1.1µm light to the measured 1427nm power is negligible. We note that at the very highest power, there appears to be some increased ASE at 1120nm. This particular piece of fiber was transitioning slightly in diameter during the draw process. The next piece of fiber cut from the spool preferentially lased at 1120nm. The pitch of the microstructure was changing in this region of the draw and became too small to completely suppress the 1120nm gain. It is likely that the fiber we report on here was similar near the input end and that significant excess ASE formed at this end of the fiber. However, this 1120nm parasitic light was attenuated by the portion of the fiber nearer the pump source, which was correctly filtering the light at these wavelengths. No significant amount of 1120nm light reached the power meter measuring the 1427nm signal. This was verified by collecting light from the spectral reflection off the power meter using a multimode fiber and monitoring the spectra with the optical spectrum analyzer, which showed the 1120nm ASE was <1% of the 1427nm signal.

Figure 11 plots amplifier gain as a function of pump power for three different launched signal powers at 1427nm. The amplifier appears to attain transparency at 4W of coupled pump power. The 11dB of fiber loss is observed for the highest launched signal power, but lower launched powers are not plotted below the lower limit of the power meter ~3mW. We note the gain at 23mW and 43mW launched power is not significantly different, this may suggest that 20mW was sufficient to saturate the amplifier, though this conclusion is somewhat in doubt given the strong parasitic ASE at 930nm. For 2.5mW launched signal power, a maximum gain of 19.3dB is measured. The measured 1120nm ASE is approximately 10x higher at this point than in the 43mW launched power case, but still <1% total power when integrated across the spectrum.

For completeness, we also characterized the 30m, 808nm pumped amplifier. 11.6 dB of gain was attained for 24mW of launched signal power (splice loss was worse in this case) or 346mW of total signal power. The maximum 808nm coupled pump power was 12W prior to the onset of parasitic lasing at 920nm. At 12W coupled pump power and 346mW signal power, there was 1236mW of total power out of the amplifier. That is, ~3/4th of the total power was at 920nm. This is significantly worse than the 880nm pump case and further illustrates the need to continuously spectrally filter the 900-950nm-wavelength band in order to attain good amplifier performance from 1360-1440nm.

We have not measured the beam quality to date. However, at 920nm the M² was less than 1.3 [25]. Our calculations indicate the mode field diameter at 1427nm to be 22µm and the

loss of the next higher order mode to be 0.5 dB/m. Future work in this area will include a beam quality measurement of the amplified light at 1427 nm.

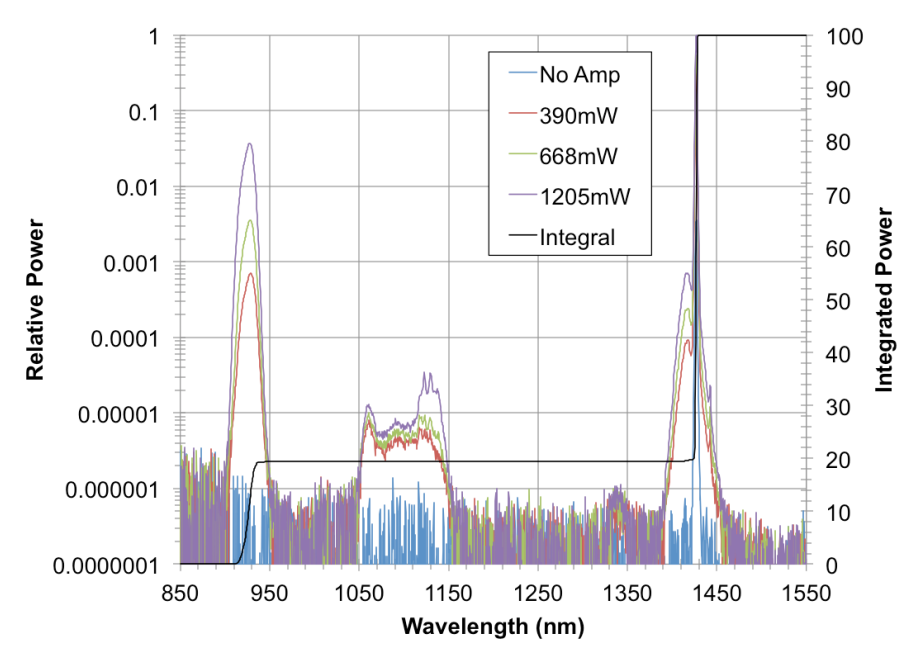


Fig. 10: Measured output spectra of 1427nm amplifier at selected power.

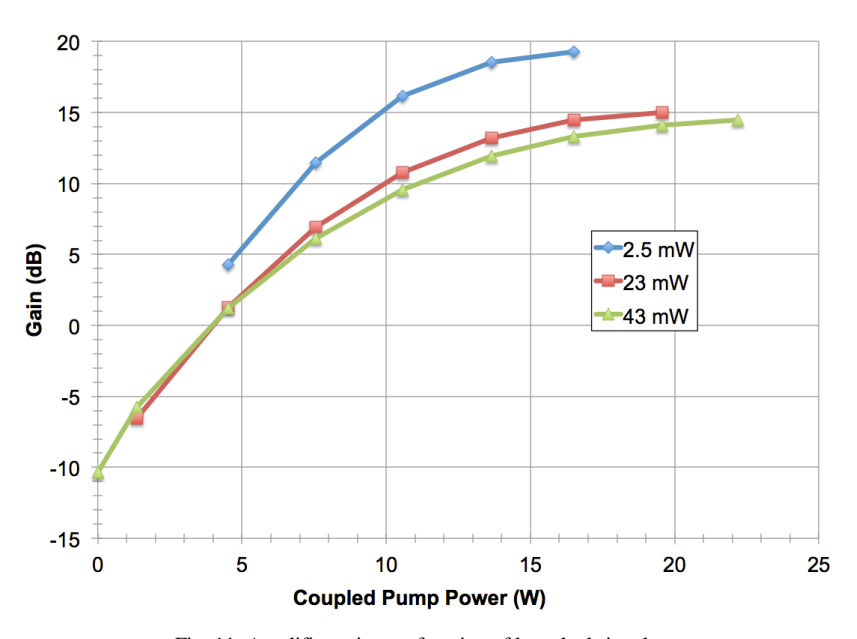


Fig. 11: Amplifier gain as a function of launched signal power.

5. Conclusions

We have experimentally demonstrated 1.2W output power at 1427nm and 19.3dB of gain at this wavelength in a neodymium fiber amplifier with a microstructure waveguide design that creates high spectral attenuation in the region from 1050-1120nm. To the best of our

knowledge this result is 100x higher than the highest average power previously attained from a neodymium fiber amplifier or laser [17, 20] and the attained gain is 9.3dB higher than any prior measurements [18]. Further our data clearly shows the potential for significant improvement in the performance of this amplifier. Key areas for future improvement are reduction of OH reducing background loss in the amplifier, expanding the waveguide spectral attenuation to cover all wavelengths from 850-1150nm, addressing the low absorption from the pump cladding (possibly by core pumping) and seeding the amplifier at a wider range of wavelengths.

Funding

The fiber reported here was fabricated under a Laboratory Directed Research and Development grant 14-ERD-078 but the specific testing reported here was funded under a grant from the LLNL Innovation Development Fund.

Acknowledgments

This work was performed under the auspices of the U.S. Department of Energy by Lawrence Livermore National Laboratory under Contract DE-AC52-07NA27344.

This document was prepared as an account of work sponsored by an agency of the United States government. Neither the United States government nor Lawrence Livermore National Security, LLC, nor any of their employees makes any warranty, expressed or implied, or assumes any legal liability or responsibility for the accuracy, completeness, or usefulness of any information, apparatus, product, or process disclosed, or represents that its use would not infringe privately owned rights. Reference herein to any specific commercial product, process, or service by trade name, trademark, manufacturer, or otherwise does not necessarily constitute or imply its endorsement, recommendation, or favoring by the United States government or Lawrence Livermore National Security, LLC. The views and opinions of authors expressed herein do not necessarily state or reflect those of the United States government or Lawrence Livermore National Security, LLC, and shall not be used for advertising or product endorsement purposes.